Journal of the Physical Society of Japan
Vol. 69, No. 1, January, 2000, pp. 276-283

Dynamical Behaviors of Periodically Forced Hindmarsh-Rose Neural Model: The Role of Excitability and 'Intrinsic' Stochastic Resonance

Yuqing WANG, Z. D. WANG and W. WANG[1]

Department of Physics, The University of Hong Kong, Pokfulam Road, Hong Kong, P.R. China
[1] *Department of Physics and Solid State Microstructure Laboratory, Nanjing University, Nanjing 210093, P.R. China*

(Received August 9, 1999)

In the presence/absence of external noise, dynamical behaviors of periodically forced neural systems and firing modes of interspike interval (ISI) are investigated by employing the Hindmarsh-Rose model. In the biologically relevant range of the forcing frequency, the interplay among the intrinsic oscillation, the forcing oscillation, and the noise leads to three kinds of firing modes: multi-modal firing, bi-modal firing, and intrinsic oscillation, in terms of which we can roughly classify the relevant experimental observations on the periodically forced sensory neural systems through their dynamical status. The resonant feature of subthreshold intrinsic oscillations shown in the ISI, the output signal-to-noise ratio, and the mean firing rate, appears to be an indication of stochastic resonance (SR) without external noise, or the 'intrinsic' SR. In the multi-modal firing region where SR leads to the skipping phenomenon, based on the 'intrinsic' SR, a possible explanation of a specific ISIH observed in experiments is given. Moreover, a neural system can tune itself to be chaotic to encode the weak signal, rather than relying only on the external noise.

KEYWORDS: neural systems, firing models, stochastic resonance

§1. Introduction

How sensory information is encoded and transmitted by neural systems has been studied for decades. Much interest on this issue has been renewed in recent years partly due to the profound understanding of stochastic resonance (SR) (see ref. 1 and references therein). SR can make use of noise to optimize the output signal-to-noise ratio (SNR) and has been demonstrated in neural systems theoretically and experimentally.[2-5] It has long been found in experiments and generally accepted that the sensory information is encoded and carried on time intervals between firings of the neuron, and the intervals have a significant random component. Such properties can be described by the interspike interval histogram (ISIH) in which the time intervals between successive spikes are assembled into a histogram. When receiving a periodic signal, the sensory neurons exhibit a kind of aperiodic firing because a random number of stimulus cycles can be skipped between successive spikes.[6-11] The ISIHs of this skipping phenomenon are polymodal. The peaks of ISIHs are roughly the multiples of the driving period and, except for the first few peaks, the envelope of the ISIH decays exponentially. The mathematical modeling of this phenomenon has been studied by a number of authors and their work mainly focused on the stochastic point processes, for example, the homogeneous Poisson point process and fractal-stochastic-point-process.[7, 12, 13] Although these models gain many insights into this phenomenon, they do not have a spiking mechanism themselves. Longtin and co-workers developed a bistable dynamic single neuron model embedded in external Gaussian white noise, and provided a simple and general explanation of the skipping phenomenon by comparing the multi-modal ISIH to the histogram of the residence time distribution of the noisy bistable system.[5] Their results indicate that the mechanism of the skipping phenomenon is SR.

Experimental and theoretical modeling studies have shown that the excitability plays an important role in neural systems.[11, 14-17] The neural system is not only situated in a noisy environment, but also can produce deterministically chaotic noise itself due to the excitability. In a recent experiment on squid giant axon, it was reported that, in the absence of external noise, the skipping phenomenon as well as the stochasticity in the multi-modal ISIH can still be observed,[18] which may originate from the deterministic chaos.[19] The subthreshold intrinsic oscillation can enhance the transduction of the weak periodic signal. This kind of enhancement can be viewed as *SR without external noise*, or the "intrinsic" SR, which gives another possible origin of aperiodicity for the multi-modal ISIH.[19, 20] In a realistic periodically-forced sensory neural system which is always in a noisy environment, whether the "intrinsic" SR can be a dynamical mechanism and how to distinguish it are not known.

On the other hand, in the experiments of sensory neural systems, the multi-modal ISIH appears merely as one part of the experimental data: many non-multi-modal ISIHs have been found.[8-11] For example, in the experiments on the cochlear nucleus neurons, the multi-modal ISIH has not been found and two types of ISIH observed are irrelevant to the period of the forcing signal.[21] How to classify or understand these modes through the dynamics and what is the role of SR in the whole dynamics

of the sensory neural system have not been clearly understood yet.

In this paper, we address the above important issues in depth. In §2, the Hindmarsh-Rose excitable neural model is presented and dynamical behaviors are analyzed. The role of the intrinsic oscillation and the interplay between it and the periodic forcing signal are elucidated. Three firing modes of the ISIH are indicated, in terms of which we are able to understand some interesting experimental results. In §3, the dynamical mechanism of the multi-modal ISIH is addressed. As well, the resonant feature and firing statistics of the "intrinsic" SR are also discussed. In §4, comparing with some experimental observations in sensory biology, the origin of noise in certain kinds of ISIH is analyzed. A possible indication of the "intrinsic" SR is also presented. The article ends with remarks and conclusions in §5.

§2. Dynamics and Classification of Isih

2.1 Model

We consider a neural system described by the Hindmarsh-Rose (HR) model.[22] This model can be considered as a generation of Fitzhugh's model,[23] but it predicts the frequency-current relationship as well as realistic waveform of the membrane potential. It is represented by the following equations:

$$\frac{\mathrm{d}X}{\mathrm{d}t} = -Y - aX^3 + bX^2 - Z + I(t) + \eta, \tag{1}$$

$$\frac{\mathrm{d}Y}{\mathrm{d}t} = c - dX^2 - Y, \tag{2}$$

$$\frac{\mathrm{d}Z}{\mathrm{d}t} = r[s(X - X_0) - Z], \tag{3}$$

$$\frac{\mathrm{d}\eta}{\mathrm{d}t} = -\frac{\eta}{t_c} + \frac{\xi(t)}{t_c}. \tag{4}$$

The neuron is characterized by three time dependent variables: the membrane potential X, the recovery variable Y, and a slow adaptation current Z. Parameters are set to be $a = 1.0$, $b = 3.0$, $c = 1.0$, $d = 5.0$, $s = 4.0$, $r = 0.006$ and $X_0 = -1.6$. Here $I(t)$ is an effective stimulus of the synaptic input and external stimulus, etc. η represents the input external noise. It is a zero-mean Ornstein-Uhlenbeck (OU) stochastic process with correlation time t_c and the autocorrelation function $\langle\eta(t)\eta(t+\tau)\rangle = (D/t_c)\exp(-\tau/t_c)$. $\xi(t)$ is the Gaussian white noise with variance D.[24] The numerical simulations are done using the fourth-order Runge-Kutta method. The time step of integration is taken as $\mathrm{d}t = 0.002\,\mathrm{ms}$, and $t_c = 0.02\,\mathrm{ms}$.

We consider a periodic driving signal as

$$I(t) = I_0 + I_1 \sin(2\pi f t), \tag{5}$$

where I_0 is the constant bias and $I_1 \sin(2\pi f t)$ is the periodic part of the signal. The constant bias I_0 can induce sub- or supra- threshold intrinsic oscillations, and can be considered as the total effective input from the external world and other neurons in the network.[19, 25] On the other hand, because I_0 is independent of time, the forms of eqs. (1)–(4) of the HR model remain unchanged if we introduce a transformation $Y' = Y - I_0$ and $c' = c + I_0$. So, changing I_0 is equivalent to changing intrinsic parameter c in eq. (2). From a viewpoint of neurobiology, a neuron can adjust its own intrinsic oscillations in response to various physiochemical stimuli.[26] Therefore, in realistic biological cases, intrinsic oscillations may be tuned by changing the total effective input of the network and/or its own neurobiological adjustment.

2.2 Classification of dynamical behaviors

As it is well known, the firing rate for $m : n$ mode-locked state, in which there are n output spikes in m forcing periods with m and n as integers, varies in a staircase pattern when I_0 and I_1 change respectively. The detailed structure has been discussed by a number of authors experimentally and theoretically.[15, 27] Below, we shall classify them from a different viewpoint which is highly useful in understanding the experimental data of periodically forced sensory neural systems.

First, we increase I_0 which represents also the intensity of the intrinsic oscillation part. For a weak periodic signal and without external noise, $I_1 = 0.1$, $f = 40\,\mathrm{Hz}$, and $D = 0$, the dynamic behavior of the system is indicated by the maximal Lyapunov exponent (λ) (Fig. 1(a)), the projection of the potential X at $t = nT(n = 1, 2, 3\cdots)$ ($T = 1/f$ is the period of the signal.) (Fig. 1(b)), and the interspike interval (ISI) (Fig. 1(c)). When I_0 increases to over the minimum firing amplitude ($I_0 = 0.98$) through a saddle-node bifurcation, the suprathreshold responses can be classified into three regions according to the firing modes of ISIH: the multi-modal region, the bi-modal region, and the intrinsic firing region, labeled as M, B and I respectively in Fig. 1. In region M, as shown in Fig. 1(c), the firing mode is the multi-modal firing: the ISIs of the chaotic firing are around nT with $n > 1$, in which the chaos is featured by positive maximum Lyapunov exponents (shown in Fig. 1(a)). In region B, the first mode-locked state is a perfect coherent state in which the system fires once at a definite phase in the time cycle of T, that is, the 1 : 1 entrainment pattern. Except for this mode, when I_0 increases, whatever the system is in a mode-locked or chaotic state, the ISIH in region B exhibits two peaks or two clusters of peaks: one with ISI being around T and the other being much smaller than T. The peak with ISI smaller than T means that, in a time cycle of T, the neuron bursts with time interval much smaller than T, which is an intrinsic feature of the neural system. For example, the mode-locked 1:n (n=2, 3, 4, 5) states can be observed in Fig. 1. All these states have approximately the same ISIH, because the period-adding only increases the number of the firing events in each time-cycle of T. When I_0 increases further, the ISIH shows only one peak which is irrelevant to the period of the forcing signal. The firing mode is intrinsic and the region is referred to as the intrinsic firing region (region I in Fig. 1). For the case of weak external noise ($D = 0.001$), the ISIs are plotted in Fig. 1(d). One can see that the three-region response pattern is still valid, except that all the mode-locked responses are messed by the noise and many less stable mode-locked states in the chaotic region (indicated by very small negative maximum Lyapunov exponents in Fig. 1(a)) disappear.

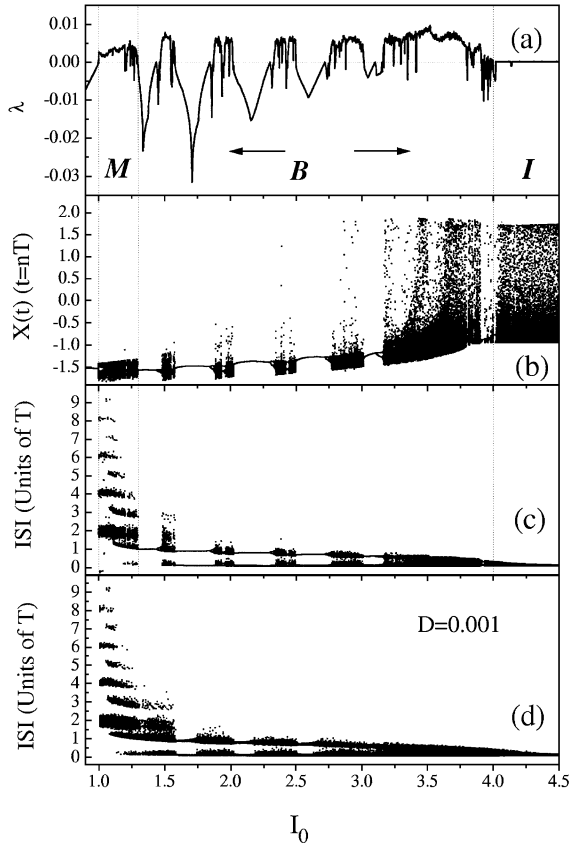

Fig. 1. The dynamical characteristics of a neuron as a function of I_0 with $I_1 = 0.1$ and $f = 40$ Hz. (a) The maximum Lyapunov exponent λ; (b) the projection of the potential $X(t)$ at $t = nT = n/f$; (c) the interspike interval ISI (in units of the period T of the forcing oscillation) and (d) in the presence of the external noise $D = 0.002$.

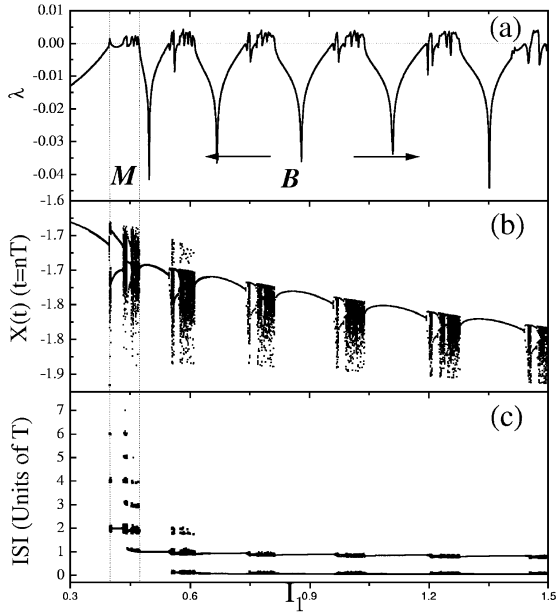

Fig. 2. The dynamical characteristics of a neuron as a function of I_1 with $I_0 = 0$, $f = 30$ Hz, and $D = 0$. (a) The maximum Lyapunov exponent λ; (b) the projection of the potential $X(t)$ at $t = nT = n/f$; (c) the interspike interval ISI (in units of the period T of the forcing oscillation).

When the periodic signal part I_1 is increased, the dynamic behavior of the system is shown in Fig. 2. The maximum Lyapunov exponent (λ), the projection of membrane potential X at $t = nT$, and the ISIs are plotted in Figs. 2(a), 2(b), and 2(c), respectively. It is seen that when I_1 increases, the response can be divided into regions M and B. Comparing Fig. 2 with Fig. 1, one can see that two M regions and two B regions have similar features. This implies that the multi-modal firing and the bi-modal firing are two regular firing modes when the periodic signal is not weak. Also the intrinsic oscillation can be evoked when the intensity of periodic signal is significant. It should be noted that there are no distinct boundaries between two neighboring regions. The change takes place gradually and the dashed lines between a pair of regions in Figs. 1 and 2 are only of symbolic significance.

The above numerical results can be understood through the dynamical status, that is, the interplay between the intrinsic oscillation and the periodic forcing oscillation. In region M, the forcing oscillation is dominant and the intrinsic oscillation is subthreshold. As a result, the chaotic ISIH has only the peaks around nT. In region B, the intrinsic oscillation becomes suprathreshold and the intrinsic firing can be observed. Therefore, both the intrinsic and forcing oscillations can be demonstrated in the ISIH. In region I, as the intensity of the intrinsic oscillation becomes so strong, together with high firing rates, that it is dominant in the ISIH.

To observe the three kinds of firing modes explicitly, the frequency of the forcing oscillation should be significantly smaller than that of the intrinsic firing. In fact, this is a specific feature of the sensory neural systems. Note that the frequency range used in the present simulation is biologically reasonable (see discussions in the end of this paper). On the other hand, the above classification is meaningful in a sense of nonlinear dynamics. It is shown that the differences among three regions can be distinguished not only from the ISI, but also from different patterns of Maximum Lyapunov exponents and projection of membrane potential, namely, the attractor patterns are different in these regions.

2.3 Three kinds of the ISIH and comparison with experimental observations

The above classification provides us a new way to classify the ISIH through its dynamical characteristics. We have examined over one hundred ISIHs obtained from a number of experiments on the periodically forced sensory neural systems, including the auditory fibers of the squirrel monkey[6] and the cat,[7] the mechanoreceptors of the macaque monkey,[8] cat retinal ganglion cells[9] and primary visual cortex,[10] and cat somatosensory neurons.[11] Although the types of these neural systems are quite different and the forcing frequency varies greatly, a large number of the ISIHs can be in principle classified according to the present classification.

Figures 3(a)–3(d) present representative ISIHs in three regions without external noise, and Figs. 3(e)–3(h) exhibit the corresponding ISIHs in the presence of weak external noise ($D = 0.002$). The multi-modal ISIHs

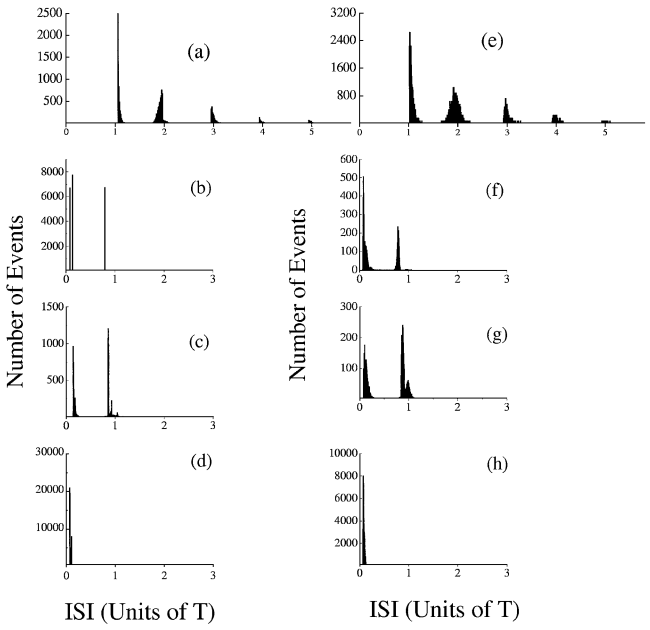

Fig. 3. $I_1 = 0.1$ and $f = 30$ Hz. The interspike interval histogram (ISIH) in the absence of external noise ($D = 0$) and (a) $I_0 = 0.95$; (b) $I_0 = 1.85$; (c) $I_0 = 2.1$; (d)$I_0 = 4.5$. The corresponding ISIHs with weak external noise ($D = 0.002$) and (e) $I_0 = 0.95$; (f) $I_0 = 1.85$; (g) $I_0 = 2.1$; (h)$I_0 = 4.5$. The ISI is in unit of the period of forcing oscillation ($T = 1/f$).

shown in Figs. 3(a) and 3(e) indicate that the peaks are around nT and each peak is broadened by the external noise. Comparing these ISIHs with escape time distribution of SR for bi-stable model,[28] they look like almost the same. In the present case, the subthreshold dynamics, or the subthreshold intrinsic oscillation plays an important role in generating the multi-modal ISIHs. While for the bistable model, there are no intrinsic oscillations, and the external noise leads to this effect. Solely from the ISIH, we can hardly determine whether the intrinsic oscillation or the external noise is dominant. This kind of ISIH has been reported in the experiments on the auditory fibers of the squirrel monkey (see Figs. 1, 3, 4, and 7 in ref. 6), the mechanoreceptors of the macaque monkey (see Figs. 11, 14, and 16 in ref. 8), the primary visual cortex of the cat (see Fig. 7 in ref. 10), and cat somatosensory neurons (see Figs. 6 and 7 in ref. 11).

Figures 3(b) and 3(f) show the 1:3 mode-locked state and the corresponding state in the presence of external noise, respectively. Figures 3(c) and 3(g) display chaotic firings in region B without and with external noise, respectively. The difference between Figs. 3(b) and 3(c) is apparent because one is a mode-locked state and the other is a chaotic state. However, in the presence of external noise, their ISIHs (see Figs. 3(c) and 3(g)) are unlikely quite different. So in the realistic experimental cases where the external noise is always present, the bimodal ISIH is featured by two peaks, which are shown in Figs. 3(c) and 3(g). This mode is observed in the experiments on the the auditory fibers of the cat,[7] the mechanoreceptors of the macaque monkey (see also Figs. 11, 14 and 16 in ref. 8), cat retinal ganglion cells (see Figs. 6, 7 and 8 in ref. 9) and cat primary visual cortex (see Fig. 2 in ref. 10).

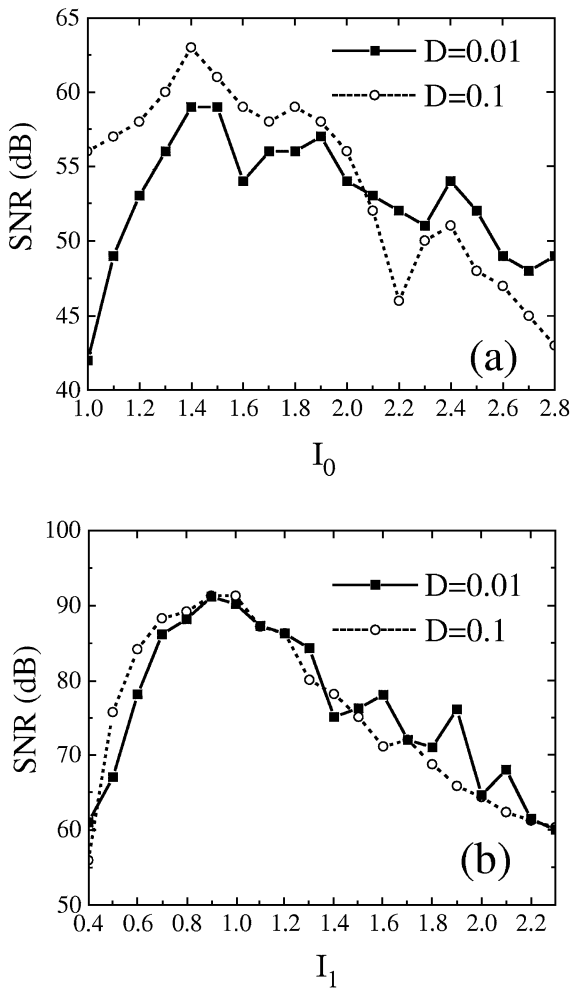

Fig. 4. (a) The signal-to-noise ratio (SNR) *vs* the constant bias I_0 with $D = 0.01$ (dashed line) and $D = 0.1$ (solid line) for $I_1 = 0.1$ and $f = 40$ Hz. (b) The SNR *vs* the intensity of signal I_1 with $D = 0.01$ and $D = 0.1$ for $I_0 = 0$ and $f = 30$ Hz.

The ISIHs in region I are shown in Figs. 3(d) and 3(h). The ISIH appears to be irrelevant to the forcing signal. The signal is contained in the spike train implicitly. This mode of ISIH was indeed observed in the experiments on mechanoreceptor of the macaque monkey (see also Figs. 11, 14 and 16 in ref. 8), and was known as 'one-type I' and 'one-type L' response modes for the cochlear nucleus neurons.[21]

Our numerical computation can simulate in detail the experimental results on the periodically driven mechanoreceptor of the macaque monkey.[8] In the experiment, the input signal consists of a sine wave part and a constant bias, as given by eq. (5). As shown in Fig. 11 of ref. 8, when the amplitude of a 40 Hz signal increases, the change of its ISI pattern is similar to Fig. 2 in detail. The three kinds of ISIH are shown in Fig. 16 in ref. 8 and resemble Fig. 3. As well, other firing features found in the experiments can also be simulated numerically, *e.g.*, the firing threshold for the sine wave signal in the experiment, as shown in Fig. 21 in ref. 8, is similar to that of the HR model (see Fig. 4 in ref. 19).

§3. Multi-modal ISIH and Stochastic Resonance

3.1 The "intrinsic" stochastic resonance

We now focus on the skipping phenomenon. As shown in Figs. 1 and 2, the multi-modal region where skipping is observed is always situated at the edge of the sub- and supra-threshold response region, which means that the signal should be weak in the multi-modal region. To understand this point, we extend the spirit of our previous work.[19] In the excitable neural system considered, even if the periodic signal is too weak to make the neuron fire, the neuron can provide subthreshold intrinsic oscillations to help it exceed the threshold, and thus induce noise due to the deterministic chaos. It has been argued that the conditions of SR are, at least, a threshold, a subthreshold signal, and noise.[1] The first two conditions are obviously present in our case, while the last one is induced intrinsically. Therefore the mechanism can be considered as SR without external noise, or the 'intrinsic' SR. In the bistable model, these three elements exist separately and can be tuned separately to see the SR phenomenon. While in the excitable system, these three elements are coupled together. For example, increasing the constant bias I_0 not only increase the intensity and change the frequency of the intrinsic oscillation, but also lowers the effective firing barrier. Even for a zero constant bias I_0, the effective barrier is different for different frequencies of the signal and, as shown in Fig. 2, the intrinsic oscillation can also be induced by the periodic forcing. Clearly, the neuron system may tune its own intrinsic feature, by varying appropriately its internal relevant parameters, to encode the information via the mechanism of the 'intrinsic' SR.

The behavior of an excitable neural system is determined by the competition between an imposed motion and an intrinsic oscillation. The resonant feature can be seen in Figs. 1(c) and 2(c). From a viewpoint of information encoding, the 1:1 entrainment pattern is considered as the full coherent state with the maximum signal-to-noise ratio (SNR). The multi-modal region is just situated between 1:1 entrainment pattern and threshold. In this region, first, the ISI is modulated by the imposed oscillation up to $n = 9$. When I_0 increases (Fig. 1(c) or I_1 increases (Fig. 2(c)), the ISI tends to concentrate on the peak of $n = 1$, and finally reach the 1:1 entrainment pattern. When either I_0 or I_1 increases further such that the system enters the bi-modal response region, the ISI is messed by the intrinsic oscillation. Note that there are mode-locked states in region M. For example, the 2:1 and 3:2 mode-locked states can be observed in Figs. 1 and 2. The input information is partially or false encoded in these states. A very weak external noise, for example, $D = 10^{-6}$, can destroy these states. So far, these mode-locked states have not been reported in the experiments of sensory neural systems.[6-11]

The resonant feature of the 'intrinsic' SR can also be seen from the SNR. For a weak signal ($I_1 = 0.1$ and $f = 40\,\mathrm{Hz}$), the SNR against the intensity of constant bias I_0 is plotted in Fig. 4(a) with $D = 0.01$ and $D = 0.1$. The SNR reaches the maximum at roughly $I_0 = 1.4$

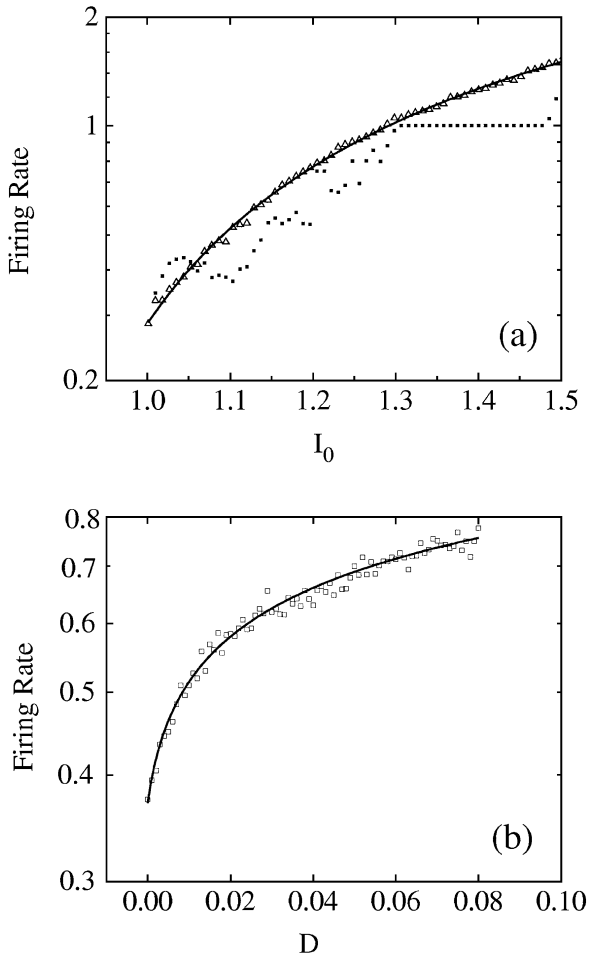

Fig. 5. $I_1 = 0.1$ and $f = 40\,\mathrm{Hz}$. (a) The mean firing rate α_0 *vs* the constant bias I_0 with $D = 0$ (solid square dots), and $D = 0.01$ (open triangle dots); the solid line represents the fitting by eq. (6). (b) The mean firing rate α_0 *vs* the external noise D with $I_0 = 1.1$ (solid square dots), the solid line represents the fitting by eq. (7).

(where the 1:1 mode-locked state exists for $D = 0$, as shown in Fig. 1(c)). When I_0 increases further, the signal is messed by the intrinsic oscillation and the SNR decreases. The coherence between the intrinsic oscillation and the forcing oscillation is also evident in that the location of maximum SNR ($I_0 \approx 1.4$) does not change for different intensities of external noise. In the absence of constant bias ($I_0 = 0$), the SNR against the intensity of the periodic signal is plotted in Fig. 4(b). When the intensity of signal increases, after reaching the maximum, the SNR will decrease. The output spike train is messed by the intrinsic oscillation due to the excitability.

3.2 The statistical feature of firing

To have a further understanding on the 'intrinsic' SR, we plot the mean firing rate α_0 versus I_0 in the multi-modal region ($\alpha_0 < 1$) in the presence/absence of external noise (Fig. 5(a)). In the absence of external noise (solid square dots), the firing rate is fixed for a mode-locked state. In particular, the statistical feature of a variety of states is extremely complicated. When a moderate external noise is added ($D = 0.01$), the mean firing rate (hollow triangle dots) can be well fitted by a simple expression

$$\alpha_0 = A_1 I_0^{\varepsilon_1} \exp[-B_1/(I_0 - C)], \tag{6}$$

with $A_1 = 3.253, B_1 = 0.508, C = 0.704$, and $\varepsilon_1 = -0.592$, which implies that the statistical feature of firing is quite different from that for $D = 0$. Figure 5(b) shows the mean firing rate α_0 versus D in the multi-modal region, which can also be fitted by another form

$$\alpha_0 = A_2(D + D_0)^{\varepsilon_2} \exp[-B_2/(D + D_0)], \tag{7}$$

where $A_2 = 1.346, B_2 = 0.0006, D_0 = 0.0062$, and $\varepsilon_2 = -0.228$. The nonzero parameter D_0 represents the contribution of chaos. It is seen from eqs. (6) and (7) that the increases of I_0 and D will have a similar effect.

From firing statistics, we can see that the role of I_0 is more complicated than that of changing the effective barrier in the HR model. In a sense of the nonlinear dynamics, one possible way to relate the firing rate with the external noise intensity and effective barrier U is the Kramers type formula $\alpha(t) = \exp[-(U/D)(1 - \eta\cos(2\pi f t))]$, where η is a constant.[16] The mean firing rate then reads

$$\alpha_0 = \langle \alpha(t) \rangle = \exp(-U/D) B_0(\eta U/D), \tag{8}$$

where B_0 is the zero-th order modified Bessel function. Comparing this equation with eq. (6), it is seen that, increasing I_0 plays a similar role of decreasing U.

The similarities between the fitting forms and Kramers-type formula imply a certain statistical feature of the neural system. When the intensity of external noise increases, the approximation of stochastic point process can work to some extend, that is why the mathematical modeling makes sense irrespective of different dynamics in connection with respectively the external noise and the deterministic chaos of the neural system in which the external noise is always present.[7, 12, 13]

§4. Chaos Versus External Noise

For most experiments, it is difficult to distinguish chaos and noise solely from some experimental data.[29] Comparing our simulation results with experimental observations on the periodically forced sensory neural systems, we can find several essential points.

First, all the mode-locked states are destroyed or messed by the external noise. The 1:1 entrainment pattern is the only mode-locked state which can be distinguished and has also been observed in the experiments on the mechanoreceptors of the macaque monkey[8] and cat retinal ganglion cells.[9] The noise component in this mode observed in the experiments comes only from the external noise, which may give a way to learn qualitatively the intensity of external noise coming from the synaptic couplings. On the other hand, the dynamic behavior of intrinsic oscillation mode when the periodically forced is essentially chaotic (see Figs. 3(d) and 3(h)), which is merely messed by the external noise.

Secondly, what is the origin of the stochasticity in the multi-modal ISIH? Because the intrinsic oscillation is subthreshold in region M, it is difficult to determine solely from the ISIH whether there is subthreshold oscillation. However, as shown in Figs. 1 and 2, in the multi-modal region, the intrinsic oscillations tend to become suprathreshold near the boundary of region M and B where the intensity of intrinsic oscillation becomes strong. The ISIHs without and with weak external noise are shown in Figs. 6(a) and 6(b) respectively. We can see that, apart from the peaks around nT, there exists a peak with ISI smaller than T. This peak stems from the intrinsic oscillation, as a direct result of the excitability of the neural system. Figure 6(c) shows the ISIH with a significant intensity of external noise, where the external noise plays a dominant role in the dynamics. Because the external Gaussian white noise has no specific frequency, the peak with ISI smaller than T shifts to the position of zero-point with a long tail, which is quite similar to that found in the bistable model subject to strong external noise (see, for example, Fig. 4 in ref. 30). As shown in Figs. 6(a)–6(c), two kinds of ISIHs may be distinguished because the intrinsic oscillation has a certain range of frequency (around 200 Hz in the present simulation). For Figs. 6(a) and 6(b) where both the intrinsic oscillation and multi-modal peaks can be clearly observed, the stochasticity comes mainly from the chaos induced by the excitability. A mixture of chaos and noise

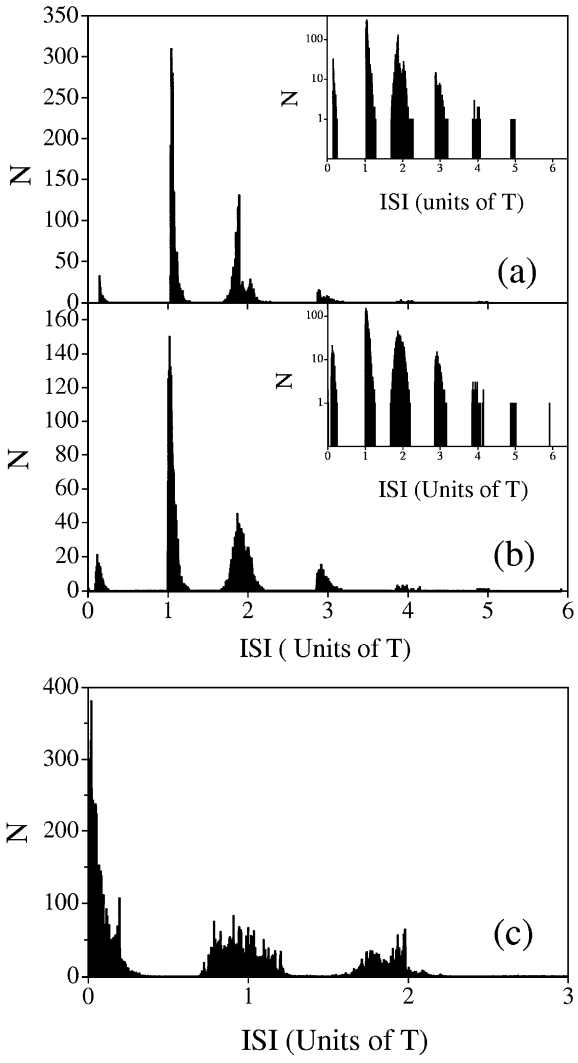

Fig. 6. The interspike interval histogram (ISIH) with $I_0 = 0.405$, $I_1 = 0.4$, $f = 40$ Hz for (a) $D = 0.0$, (b) $D = 0.002$, and (c) $D = 0.35$. N is the number of spikes per bin. Insets of (a) and (b): the same data is plotted in logoscale to show the envelope respectively.

underlies Fig. 6(c), with the noise as a dominant factor.

The ISIHs which resemble Figs. 6(a) and 6(b) have been found in the experiments on the periodically forced auditory fibers of the squirrel monkey (see Figs. 3 and 4 in ref. 6), the somatosensory neurons of the cat (see Fig. 7 in ref. 11). Since SR in the bistable or other excitable models with Gaussian white noise unlikely lead to this kind of ISIH,[31] it is possible that the first peak in the experiment results from the intrinsic oscillation, although the possibility due to the colored noise may not be excluded. On the other hand, some of the ISIHs from the cat retinal ganglion cell (see Fig. 8 in ref. 9 and the cat primary visual cortex (see Fig. 7 in ref. 10) resemble Fig. 6(c), where the effect of the external noise is stronger than that of the subthreshold intrinsic oscillation. Actually, in many experimental cases, the peak with ISI smaller than T in multi-modal ISIHs may be understood as the intrinsic oscillation messed by a moderate external noise, a possible indication of the 'intrinsic' SR, which resembles Fig. 6(b).

§5. Remarks and Conclusions

Previous studies classified the ISIHs merely in terms of their detail distributions or shapes.[12, 21] Here, for the periodically forced sensory neural systems, the ISIHs are classified by their dynamical status, that is, the interplay among the dynamical factors: the excitability, the input signal, and the noise. The three kinds of ISIHs, i.e., multi-modal firing, bi-modal firing, and intrinsic oscillation, imply three different dynamical characteristics, as well as different patterns of information encoding. Such theoretical classification actually describes well the ISIHs observed in some experiments on the periodically forced sensory neural systems, such as, the auditory fibers of the squirrel monkey[6] and the cat,[7] the mechanoreceptors of the macaque monkey,[8] cat retinal ganglion cells[9] and primary visual cortex,[10] and cat somatosensory neurons.[11]

In the multi-modal region, the SNR increases when the external noise and/or intrinsic oscillation increase, that is, the enhancement can be expected as long as the dynamical status falls in this region. The multi-modal region can also be referred to as SR region, where the signal is weak and noise and/or subthreshold intrinsic oscillation are needed to help the neuron fire the spike train. As demonstrated in the present simulation and the experiments on the periodically forced sensory neural systems, multi-modal ISIHs are a part of the whole dynamical response modes and SR can be considered as a common phenomenon in sensory biology.[1]

According to a conventional wisdom, the hearing and visual ability is surely increased when the environment noise decreases. In this sense, although the external noise can not be removed completely, the neural system may not rely solely on the external noise to encode the weak signal. Instead, the neuron can tune itself through its own physiochemical adjustment and/or total effect of the network to be chaotic to encode the information, and a part of noise in the noisy neural system comes from chaos produced by the neural system itself.

In our simulation, the chosen frequency of the forcing signal is always smaller than the frequency of intrinsic oscillation. This choice has a neurophysiological consideration and can be viewed as a specific feature of neural systems. For the sensory neural systems, there exists a most sensitive range of the forcing frequency. We have found that, although this range varies from type to type, their corresponding intrinsic oscillation frequency can always be adjusted to be higher through its own physiochemical adjustment. In the present simulation, the parameters in eqs. (1)–(4) are common for the HR model. Its sensitive frequency range is 5–70 Hz with the most sensitive frequency around 40 Hz,[19] while the intrinsic oscillation is around 200 Hz.[34] For the Hodgkin-Huxley model, the frequency of its intrinsic oscillation range from approximate 50 Hz to 170 Hz (for a constant bias changing from $6.2\,\mu\mathrm{A/cm^2}$ to $154.5\,\mu\mathrm{A/cm^2}$). This feature leads to not only the explicit three kinds of the ISIH, but also the similar dynamical behaviors of the intrinsic oscillation and the external noise. It is quite possible that this kind of adjustment may work in sensory biology.

Finally, it is worthy to point out that the dynamical firing features presented here are worked out by using the HR model, which may not be very suitable for all the periodically forced neural systems reported in refs. 6–11. However, the classification of the ISIH appears to be applicable more widely. For example, we have also done some simulations based on the Hodgkin-Huxley model and have observed similar feature of the firing, such as the multi-modal ISIH in the absence of external noise, three kinds of firing modes and its corresponding different patterns of information transmission, and the most sensitive firing frequency range. In our opinion, in spite of different excitable neuron models, their physical origin and essential dynamical feature under the periodic stimulation are basically similar.

Acknowledgments

This work was supported by a CRCG grant at the University of Hong Kong. W. Wang acknowledges the support by the Outstanding Young Research Foundation of the National Natural Science Foundation (Grant No. 19625409).

1) L. Gammaitoni, P. Hänggi, P. Jung and F. Marchesoni: Rev. Mod. Phys. **70** (1998) 223.
2) J. K. Douglass, L. Wilkens, E. Pantazelou and F. Moss: Nature **365** (1993) 337.
3) K. Wiesenfeld and F. Moss: Nature **373** (1995) 33; J. E. Levin and J. P. Miller: Nature **380** (1995) 165; B. J. Gluckman *et al.*: Phys. Rev. Lett. **77** (1996) 4098; S. M. Bezrukov *et al.*: Nature **378** (1995) 362; P. Cordo *et al.*: Nature **383** (1996) 769; J. J. Collins *et al.*: Nature **383** (1996) 770.
4) A. R. Bulsara and G. Schmera: Phys. Rev. E **47** (1993) 3734; A. R. Bulsara *et al.*: Phys. Rev. E **49** (1994) 4989; J. J. Collins, *et al.*: Nature **376** (1995) 236; A. R. Bulsara *et al.*: Phys. Rev. E **53** (1996) 3958.
5) A. Longtin, A. R. Bulsara and F. Moss: Phys. Rev. Lett. **67** (1991) 656; A. Longtin, A. R. Bulsara, D. Pierson and F. Moss: Biol. Cybern. **70** (1994) 569.
6) J. Rose, J. Brugge, D. Anderson and J. Hind: J. Neurophysiol. **30** (1967) 769.
7) N. Y. S. Kiang: *Handbook of physiology, Vol. III*, (American Physiological Society, 1984) Part 2, Chap. 15, p. 639.

8) W. H. Talbot, I. Darian-Smith, H. H. Kornhuber and V. B. Mountcastle: J. Neurophysiol. **31** (1968) 301.
9) T. Ogawa, P. O. Bishop and W. R. Levick: J. Neurophysiol. **6** (1966) 2.
10) R. Siegel: Physica D **42** (1990) 385.
11) D. R. Chialvo and A. V. Apkarian: J. Stat. Phys. **70** (1993) 375.
12) H. C. Tuckwell: *Stochastic Processes in the Neurosciences*, (Society for Industrial and Applied Mathematics, Philadelphia, Pennsylvania, 1989).
13) S. B. Lowen and M. C. Teich: J. Acoust. Am. **92**(2) (1996) 803; M. C. Teich, R. G. Turcott and R. M. Siege: IEEE Engineering in Medicine and Biology Magazine **15** (1996) 79; A. R. Kumer and D. H. Johnson: J. Acoust. Soc. Am. **93** (1993) 3365; J. Li and E. D. Young: Hear. Res. **69** (1993) 151; E. D. Young and P. E. Barta: J. Acoust. Soc. Am. **79** (1986) 426.
14) K. Schäfer, H. A. Braun and L. Rempe: Prog. Brain. Res. **74** (1988) 29; H. Braun, H. Wissing, K. Schäfer and M. C. Hirsh: Nature **367** (1994) 270; E. Pantazelou, C. Dames, F. Moss, J. Douglass and L. Wilkens: Int. J. Bifurc. Chaos **5** (1995) 101.
15) N. Takashi, Y. Hanyu, T. Musha, R. Kubo and G. Matsumoto: Physica D **43** (1990) 318.
16) K. Wiesenfeld, D. Pierson, E. Pantazelou, C. Dames and F. Moss: Phys. Rev. Lett. **72** (1994) 2125.
17) D. R. Chialvo, A. Longtin and J. Mäller-Gerking: Phys. Rev. E **55** (1997) 1798; J. J. Collins, C. C. Chow and T. T. Imhoff: Phys. Rev. E **52** (1995) R3321; W. Wang and Z. D. Wang: Phys. Rev. E **55** (1997) 7379; A. Longtin: Phys. Rev. E **55** (1997) 868.
18) D. T. Kaplan, J. R. Clay, T. Manning, L. Glass, M. R. Guevara and A. Shrier: Phys. Rev. Lett. **76** (1996) 4074.
19) W. Wang, Y. Wang and Z. D. Wang: Phys. Rev. E **57** (1998) R2527.
20) R. Benzi, A. Sutera and A. Vulpiani: J. Phys. A: Math. Gen. **14** (1981) L453; V. S. Anishchenko, A. B. Neiman and M. A. Safanova: J. Stat. Phys. **70** (1993) 183.
21) D. R. F. Irvine: *Progress in Sensory Physiology 7: The Auditory Brainstem*, ed. H. Autrum, D. Ottoson, E. R. Perl, R. F. Schmidt and W. D. Willis (Springer-Verlag, 1986) Chap. 4.
22) J. L. Hindmarsh and R. M. Rose: Nature **296** (1982) 162; Proc. R. Soc. London B **221** (1984) 87; *ibid.* **225** (1985) 161.
23) R. Fitzhugh: Biophys. J. **1** (1961) 445.
24) P. V. E. McClintock and F. Moss: *Noise in nonlinear dynamical systems*, ed. F. Moss and P. V. E. McClintock (Cambridge University Press, Cambridge, England, 1989) Vol. 3, p. 243.
25) W. Wang, G. Perez and H. A. Cerdeira: Phys. Rev. E **47** (1993) 2893.
26) *The Neuron: Cell and Molecular Biology*, ed. I. B. Levitan and L. K. Kaczmarek (Oxford University Press, 1991).
27) *Chaos in Biological Systems*, ed. H. Degn, A. V. Holden and L. F. Olsen (Plenum, New York, 1987).
28) T. Zhou and F. Moss: Phys. Rev. A **42** (1990) 3161.
29) L. Glass and M. C. Mackey: *From Clocks to Chaos: The Rhythms of life* (Princeton University Press, 1988).
30) A. R. Bulsara and L Gammaitoni: Physics Today **49** (1996) 39.
31) We also examined the Hodgkin-Huxley model with white noise, and find that the conventional SR lead to the first peak at zero-point in the ISIH.
32) Y. Wang, Z. D. Wang and W. Wang: J. Phys. Soc. of Jpn. **67** (1998) 3637.
33) A. V. Holden and Y. S. Fan: Chaos, Soliton & Fractals **2** (1992) 221; *ibid.* **2** (1992) 349.
34) Note that these frequencies can also be tuned by changing parameter r in eq. (3) to fit other kinds of neural systems.[27, 32, 33)]